Contrast Leakage Patterns from Dynamic Susceptibility Contrast Perfusion MRI in the Grading of Primary Pediatric Brain Tumors

Chang Y. Ho, Jeremy S. Cardinal, Aaron P. Kamer, Chen Lin, Stephen F Kralik

Indiana University School of Medicine

Department of Radiology

Corresponding author:

Chang Ho

705 Riley Hospital Drive

MRI department

Indianapolis, IN 46202

cyho@iupui.edu

A portion of this work was presented at the ASNR 2014 annual meeting in Montreal, Canada

This is the author's manuscript of the article published in final edited form as:
Ho, C. Y., Cardinal, J. S., Kamer, A. P., Lin, C., & Kralik, S. F. (2016). Contrast Leakage Patterns from Dynamic Susceptibility Contrast Perfusion MRI in the Grading of Primary Pediatric Brain Tumors. American Journal of Neuroradiology, 37(3), 544–551. https://doi.org/10.3174/ajnr.A4559

PURPOSE: To evaluate contrast leakage patterns from dynamic susceptibility contrast (DSC) tissue signal intensity time curves (TSITC) in grading pediatric brain tumors.

MATERIALS AND METHODS: A retrospective review of TSITCs from 63 cases of pediatric brain tumors with preoperative DSC perfusion MRI was performed independently by two neuroradiologists. TSITCs were generated from ROIs placed in the highest perceived tumor rCBV. The post-bolus portion of the curve was independently classified as returning to baseline, continuing above baseline (T1-dominant contrast leakage), or failing to return to baseline (T2*-dominant contrast leakage). Inter-observer agreement of curve classification was evaluated using Cohen's kappa. A consensus classification of curve type was obtained in discrepant cases, and the consensus classification was compared with tumor histology and World Health Organization grade.

RESULTS:

TSITC classification concordance was 0.69 (0.54 – 0.84) overall, and 0.79 (0.59 – 0.91) for a T1-dominant contrast leakage pattern. 25/25 tumors with consensus T1-dominant contrast leakage were low grade (PPV, 1.0; 0.83–1.00). By comparison, tumors with consensus T2*-dominant contrast leakage or return to baseline were predominantly high grade (10/15 and 15/23 respectively) with a high negative predictive value (1.0; 0.83-1.0). For pilomyxoid or pilocytic astrocytomas, a T1-dominant leak demonstrates high sensitivity (0.91; 0.70-0.98) and specificity (0.90, 0.75-0.97).

CONCLUSION:

There is good inter-observer agreement in classification of DSC perfusion TSITCs for pediatric brain tumors, particularly for T1 dominant leakage. Among pediatric brain tumor patients, a T1-dominant leakage pattern is highly specific for a low grade tumor, and demonstrates high sensitivity and specificity for pilocytic or pilomyxoid astrocytomas.

ABBREVIATIONS: DSC = dynamic susceptibility contrast; ROI = region of interest; rCBV = relative cerebral blood volume; WHO = World Health Organization

INTRODUCTION

Primary brain tumors represent 29% of all childhood cancers, are the most common solid childhood tumor, and are the leading cause of cancer death in this age population [1]. With experienced pediatric neuroimaging specialists, presurgical diagnosis with anatomic MRI sequences can be accurate, especially with a classic appearance and location presentation. However, many primary neoplasms do not follow the classic imaging appearance and the use of advanced imaging techniques such as perfusion imaging, diffusion weighted imaging, and MR spectroscopy have been utilized to grade primary pediatric tumors [2-4].

Dynamic susceptibility contrast (DSC) perfusion MRI has demonstrated utility in the pretreatment evaluation of adult intracranial neoplasms for tumor grading, guiding biopsy, and prognosis. However, while the most common adult primary parenchymal neoplasms are of the astrocytic cell type, the most common pediatric primary brain tumors have diverse cellular origins, with astrocytic origin for pilocytic astrocytomas and embryonal neuroepithelial origin for medulloblastomas. Even within astrocytomas, outside of the classic "cyst and mural nodule" appearance of pilocytic astrocytomas, there is some overlap in the radiographic and histological appearance of pilocytic astrocytomas and high grade gliomas, with relative cerebral volume (rCBV) demonstrating usefulness in distinguishing the two astrocytic entities [5]. However, when the most common pediatric primary brain tumors are evaluated, there is an overlapping range of rCBV values, particularly between pilocytic astrocytomas and medulloblastomas, limiting the usefulness of DSC perfusion in predicting low versus high grade tumors preoperatively [2].

While rCBV has received the greatest attention in differentiating tumor grades from perfusion imaging in adult tumors [6-8], tissue signal intensity time curves (TSITC) have also demonstrated diagnostic utility, most notably in differentiating primary CNS lymphoma from glioblastoma multiforme and metastases [9-11]. We evaluate the inter-observer agreement of classification of DSC perfusion MRI TSITCs and the utility of curve classification as a tool for grading pediatric brain tumors.

MATERIALS AND METHODS

Following institutional review board approval, a retrospective radiology database search from September 2009 to August 2013 identified a total of 65 pediatric brain tumor patients with pathology-proven diagnosis and assigned World Health Organization (WHO) grade who had undergone DSC perfusion MRI on initial evaluation prior to chemotherapy, biopsy or surgical resection. In the majority of cases, a single dose of 2mg/kg IV dexamethasone was given emergently prior to MRI for the treatment of tumor associated cerebral edema. A total of two cases were excluded for a total of 63 cases for review. One case was excluded due to poor contrast bolus and the second case was excluded due to significant susceptibility artifact generated by the patient's dental braces. This study population was previously reported [2].

MR Imaging

DSC perfusion MR images were obtained during the first pass of a bolus of gadobenate dimeglumine (MultiHance, Bracco Diagnostics Inc., Princeton, NJ) on 1.5T and 3T MRI scanners (Siemens Avanto and Verio, Erlangen, Germany) using a gradient echo echo planar sequence (TR 1410-2250 / TE 30 and 45 ms, flip angle 90 degrees). Two different TEs were utilized on different scanners. A range of TR was adjusted for tumor coverage. No cases were performed with a preload of IV contrast. Following a pre-contrast phase to establish a baseline, a contrast medium dose of 0.1 mmol/kg of body weight was injected followed by a normal saline flush for a total volume of 32 ml. When possible, an 18 or 20 gauge peripheral intravenous access was used with a power injector rate of 5 ml/s. In some cases, primarily with smaller children, only 24 gauge peripheral intravenous access was possible. Contrast bolus adequacy was evaluated by two fellowship-trained board-certified neuroradiologists with certificate of added qualification (C.H., 7 years experience, and S.K., 3 years experience) based on TSITCs and included or excluded in consensus.

Data Analysis

Using a commercially available workstation (Dynasuite Neuro 3.0, InVivo Corp, Pewaukee WI), each neuroradiologist independently selected multiple 3 to 5 mm^2 ROIs within the tumor, placed at the locations of perceived highest rCBV using Dynasuite-generated rCBV maps, blinded to pathologic diagnosis. Anatomic MR imaging sequences were used to help define tumor location and avoid major blood vessels or hemorrhage when placing the ROI. The resulting signal intensity curve from the ROI with the highest rCBV was used for classification. This technique has been previously described in the literature [2]. Use of the maximum rCBV for characterization of the TSITC ensures that the most perfused portion of a heterogeneous tumor is evaluated, reducing sampling errors. Curves were assessed out to 50 TRs on the time axis. A Y-axis value prior to the first pass bolus was chosen to represent the average of the baseline and compared to the final Y axis value at 50TRs. The portion of the curve following the first pass of contrast medium bolus was characterized as returning to a level within ± 10% of baseline with plateau (return to baseline Figure 1), overshooting at least 10% above baseline without plateau (T1-dominant contrast leakage; Figure 2), or failing to return to a level less than 10% below baseline (T2*-dominant contrast leakage; Figure 3). Inter-observer agreement was assessed using Cohen's kappa. Blinded consensus opinion was obtained in cases with discrepant curve classification, and the resulting TSITCs were compared with individual WHO tumor grade. TSITC results were also compared to the averaged rCBV maximum between the two observers. Histopathologic evaluation of surgical specimens for all tumors was performed by one of two board-certified neuropathologists who determined a diagnosis and assigned a WHO grade of I through IV.

A Chi-square test of independence was used to assess for potential significant differences between 1.5T and 3.0T, 30ms and 45ms TE, range of TR, and dexamethasone administration. Diagnostic accuracy was assessed for specific curve patterns.

Statistical analysis was performed using SPSS 21 (IBM Corp. Armonk, NY) and an online statistical calculator (Vassarstats, http://vassarstats.net/).

RESULTS

Patient characteristics are summarized in table 1. There were 38 low grade (WHO grade I-II) tumors, and 25 high grade (WHO grade III-IV) tumors.

Independent classification of TSITCs by two neuroradiologists had a Cohen's kappa of 0.69 (0.54 – 0.84) indicating good inter-observer agreement. Proportion of agreement was highest with T1-dominant pattern (0.79, 0.56-0.91) compared to T2*-dominant pattern (0.60, 0.39-0.78) and return to baseline (0.57, 0.35-0.76).

The Chi-squared test for independence between 1.5T and 3.0T scanners (p=0.63), 30 and 45 TE (p=0.55), and TR range (p=0.14) failed to show significance indicating that the null hypothesis is not rejected, or, that leakage patterns are not dependent on the differences in magnet strength, TE or TR in our scanning parameters. Dexamethasone, however did show some significant (p=0.02) effect. Further Chi-squared analysis between tumors treated with dexamethasone (N=41) and without dexamethasone (N=22) showed a significant difference in all low grade tumors (p=0.03) but not with pilocytic astrocytomas (p=0.99), pilomyxoid astrocytomas (p=1.0) or both of the piloid tumors together (p=0.46). For high grade tumors, dexamethasone also did not show a significant effect (p=0.09).

All tumors

Among 38 low grade tumors, twenty-five had consensus classification of T1-dominant contrast leakage while thirteen had a consensus curve classification other than T1-dominant leakage--either return to baseline or T2*-dominant leakage. The 25 tumors with T1-dominant contrast leakage included: 15 pilocytic astrocytomas, six pilomyxoid astrocytomas, one low grade glioneuronal tumor, one WHO grade 2 ependymoma, one desmoplastic infantile ganglioglioma, and one choroid plexus papilloma. Tumors showing a consensus curve classification with T2*-dominant leakage or return to baseline were predominantly high grade. Ten out of 15 tumors identified as having post-bolus curve with T2*-dominant leakage were high grade (positive predictive value, 0.67, 0.39 – 0.87), and 15 out of 23 tumors with curves identified as returning to baseline were high grade (positive predictive value, 0.65, 0.43 – 0.83). Combining T2* and return to baseline patterns for high grade tumor yielded high sensitivity (1.0, 0.83-1.0) and negative predictive value (1.0, 0.83-1.0) at the cost of specificity (0.66, 0.49-0.80). The most common high grade tumors such as medulloblastoma, anaplastic ependymoma, and glioblastoma had both T2* and baseline patterns. All three cases of atypical teratoid rhabdoid tumor showed a return to baseline pattern. Conversely, the most common low grade tumors such as pilocytic astrocytoma and pilomyxoid astrocytoma demonstrated predominantly T1-dominant leakage: 15/17 for pilocytic astrocytoma and 6/6 for pilomyxoid astrocytoma. One case out of three WHO II ependymomas showed T1-dominant leakage. For the diagnosis of pilocytic or pilomyxoid astrocytoma, a T1-dominant leakage pattern yields a high sensitivity (0.91, 0.70-0.98; negative predictive value, 0.95, 0.81-0.99) and specificity (0.90, 0.75-0.97; positive predictive value, 0.84, 0.63-0.95) [Table 2].

An analysis of variance (ANOVA) showed no significant differences ($p=0.11$, F-ratio=2.32) between the means of the rCBV maximum for each leakage pattern (T1-dominant = 3.25 ± 3.3, Baseline = 3.25 ± 2.2, T2*-dominant =5 .18 ± 3.6). A T-test between the means of rCBV maximum for T1-dominant leakage (3.25 ± 3.3) and T2*-dominant combined with baseline leakage patterns (4.02 ± 2.93) also yielded no significant difference ($p=0.33$). Chi squared tests were performed for significant differences between WHO grade and TSITC leakage results. Grade I versus grade II tumors were not significant ($p=0.38$) nor was grade III versus grade IV tumors ($p=0.93$). Only high (III and IV) versus low grade (I and II) were significant ($p<0.0001$).

Dexamethasone group

Among the forty-one patients with tumors that received dexamethasone prior to DSC perfusion MRI, nineteen had consensus T1-dominant leakage, twelve had a consensus T2*-dominant leakage pattern, and ten had a consensus return to baseline pattern. All nineteen with a T1-dominant leakage pattern were low grade tumors while five other low grade tumors had a leakage pattern other than T1-dominant leakage. Out of twelve tumors with T2*-dominant leakage, nine were high grade. Out of ten tumors with return to baseline pattern, eight were high grade. Thirteen out of fourteen pilocytic astrocytomas and three out of three pilomyxoid astrocytomas demonstrated T1-dominant leakage. Diagnostic accuracy for this cohort is summarized in table 2. Within the entire dexamethasone group, no significant differences were seen between magnet strengths ($p=0.62$), TE ($p=0.32$), or TR ($p=0.20$).

No Dexamethasone group

Among the twenty-two patients with tumors that did not receive dexamethasone prior to DSC perfusion MRI, six had a consensus T1-dominant leakage, three had a consensus T2*-dominant leakage, and thirteen had a consensus return to baseline pattern. All six tumors with a T1-dominant leakage pattern were low grade tumors. Eight low grade tumors had a leakage pattern other than T1-dominant leakage. Out of three tumors with T2*-dominant leakage, only one was high grade. Out of thirteen tumors with return to baseline pattern, seven were high grade. Two out of three pilocytic astrocytomas and three out of three pilomyxoid astrocytomas demonstrated T1-dominant leakage. Diagnostic accuracy is summarized in table 2. Within the entire no dexamethasone group, no significant differences were seen between magnet strengths ($p=0.08$), TE ($p=0.97$), or TR ($p=0.40$).

DISCUSSION

In practice, hemodynamics, status of the blood-brain barrier, timing of the contrast bolus, and MR pulse sequence parameters affect the shape of the TSITC [12-16]. Disruption or lack of a blood-brain barrier results in leakage of contrast medium into the extravascular extracellular space. While in the intravascular space, paramagnetic contrast medium causes predominantly T2* effects with loss of MR signal, however once in the extravascular extracellular space, T1-shortening effects compete with the T2* effects [15, 16]. Depending on the MR parameters and biological tissue environment, T1-shortening effects may predominate and cause a post bolus

curve that returns to and then passes baseline, or T2* effects may predominate and result in a post bolus curve that fails to return to baseline [15]. Another mechanism for a curve that fails to return to baseline was suggested by Kassner et al who showed that residual T2* effects may reflect delayed passage of intravascular contrast medium due to vascular tortuosity, disorganization, and hypoperfusion in areas of increased neovascularity, comparing this effect to the tumor staining seen on catheter angiography [13].

Previous authors describe the portion of the curve after the peak as percent signal recovery, [9, 17] with a high percent signal recovery correlating with our T1-dominant leakage, and a low percent signal recovery as T2*-dominant leakage, or with smaller T2* effects, a return to baseline. Cha et al. demonstrate a significant difference between metastatic brain tumors and glioblastoma as well as the associated surrounding abnormal white matter in adults with greater T2* effects and less than 50% return to baseline for metastatic tumors compared to greater than 75% recovery for glioblastoma. They suggest that this difference is due to the lack of a blood brain barrier leading to greater uniform vascular permeability and leakage in metastatic tumors, compared to some presence of a blood brain barrier in glioblastomas, with less uniform vascular permeability [15]. Lastly, the balance between T1 and T2* effects is affected by varying MR parameters including the flip angle, TE and TR in gradient echo EPI DSC perfusion MRI [10, 12, 13, 15, 16, 17]. We used a narrow range of TE for similar T2* effect across scanners and a uniform flip angle on all scanners for recovery from the peak. Previous authors have used a low flip angle to suppress T1 signal effects [16, 17]; however in our study, our 90 degree flip angle does not sufficiently suppress the T1 signal for our range of TR to prevent overshoot of the baseline in most low grade tumors, which we categorized as T1-dominant leakage.

Advances in knowledge

A striking finding in our data was 100% positive predictive value (25 of 25) for low grade tumors if a T1-dominant leakage pattern was identified. The converse is also true in that the lack of a T1 leak pattern (T2* or return to baseline) results in a 100% negative predictive value for high grade tumors. T1-dominant leakage patterns were also sensitive and specific for either a pilocytic astrocytoma or pilomyxoid astrocytoma. In addition, good interobserver agreement for identifying a T1-dominant leakage pattern was found, indicating significant potential clinical utility for grading pediatric brain tumors with TSITCs from DSC perfusion.

Little prior data exists in the literature regarding the use of DSC perfusion MRI and signal intensity curves in the evaluation of pediatric brain tumors. Similar to our findings, Grand et al reported a series of 9 pilocytic astrocytomas evaluated with DSC perfusion MRI, in which all 9 tumors demonstrated an overshoot of the baseline, or T1-dominant contrast leakage pattern [16]. Cha reported that pilocytic astrocytomas have > 70% signal recovery, while medulloblastomas have < 50% signal recovery, which is consistent with our findings [18].

Prior to our study, a T1-dominant leakage pattern has most notably been demonstrated in primary CNS lymphoma, and has been shown to be useful in distinguishing lymphoma from glioblastoma multiforme and CNS metastases [9-11]. Despite the lack of neoangiogenesis in CNS lymphoma, both glioblastoma and lymphoma have elevated rCBV, but have a significant

difference in the high percent signal recovery for lymphomas. This has been attributed to the characteristic perivascular invasion of lymphoma cells, leading to disruption of the basement membrane and resulting vascular permeability. The hypercellularity of lymphoma with a small extravascular extracellular space has been suggested as a contributing factor although the exact mechanism for T1-dominant leakage effects in lymphoma is not well understood [9]. This finding contradicts the findings of Cha et al. in that the lack of a blood brain barrier in metastatic disease, with resulting vascular permeability results in a low percent recovery, or T2*-dominant effect rather than the T1-dominant effect in CNS lymphoma [9, 17]. Cha et al. used a flip angle of 35° compared to 80° for Mangla et al., which may contribute to the differing TSITC results. Biological factors may include differing rates of contrast leakage between CNS lymphoma and metastatic disease with a faster accumulation and concentration of extravascular contrast in metastatic disease leading to T2*-dominant effects. The mechanism underlying the observed post-bolus T1-dominant effects in low-grade pediatric brain tumors is not known, but is also likely related to the balance between T1-shortening and T2* effects of paramagnetic contrast medium that has leaked into the extravascular extracellular space. Other factors affecting the T1-T2* balance may include characteristics of the extravascular space such as cellular density, water content, and other molecular constituents, in addition to hemodynamic flow issues and capillary permeability.

Pilocytic astrocytomas and pilomyxoid astrocytomas account for 21 of the 25 tumors in our series demonstrating post-bolus T1-dominant leakage. Pilocytic astrocytomas are described as having biphasic histology with areas of loose glial tissue interposed with compacted piloid tissue composed of dense hypercellular sheets of elongated bipolar cells [20]. Distinguishing features of pilomyxoid astrocytomas include monomorphous piloid cells in a myxoid background with an angiocentric pattern, similar to perivascular pseudorosettes in ependymomas. While pilomyxoid astrocytomas tend to occur in younger children in the hypothalamic/ chiasmatic pathway, with more aggressive behavior, and a higher propensity for leptomeningeal spread, pilocytic and pilomyxoid astrocytomas have significant morphological and imaging overlap. There have been reports of recurrent pilomyxoid tumors demonstrating pilocytic features after several years, with some authors suggesting that pilomyxoid astrocytoma may be an infantile form versus an extreme subtype of pilocytic astrocytoma [21-23]. It is because of this significant overlap, and the lack of distinguishing imaging characteristics between the two tumors that we calculated diagnostic accuracy with both tumors rather than separately. Vascular proliferation can be seen in the solid component of both tumors but with more mature endothelial cells in a single layer compared to glioblastomas [24, 25]. These single endothelial layers with open tight junctions and fenestrae as well as hyaline degeneration around vessels have been postulated to allow contrast medium extravasation and therefore vascular permeability [18]. Similar to CNS lymphomas, this level of increased vascular permeability likely plays a partial but crucial role in the T1-dominant leakage effects seen in both tumors. Further research between different pediatric tumors using T1 signal based dynamic contrast enhancement MRI may be helpful in elucidating differences in vascular permeability.

Affect of Dexamethasone on leakage patterns

We could not control for the administration of dexamethasone on newly diagnosed brain tumor pediatric patients as corticosteroids are a first line emergent therapy for controlling the cerebral swelling and the resultant mass effect from mass occupying brain tumors. In a previous work on the same patient population, there was no significance between patients with and without dexamethasone treatment and rCBV measurements [2]. However, given the known rapid effects of dexamethasone in decreasing capillary permeability and reducing vasogenic edema [26, 27], the significance between patient populations is not surprising. However, only our low grade tumor group was significant, and there was larger proportion of T1-dominant and T2*-dominant leakage patterns within the dexamethasone group. This result seems counterintuitive as high grade tumors typically have greater vasogenic edema and mass effect, and decreasing capillary permeability should trend toward the return to baseline pattern, as this pattern would best represent no leakage. In reality, multiple physiological parameters likely affect the leakage pattern as indicated by our results. Despite the significance of dexamethasone on the low grade tumor group, the 100% specificity of a T1-dominant leakage pattern for low grade pediatric tumors and high sensitivity and specificity for piloid astrocytomas remain unchanged for both groups with or without dexamethasone.

Implications for patient care

Despite uncertainty in the exact underlying mechanism, a T1-dominant contrast leakage pattern on the signal intensity curve obtained in the region of highest tumor rCBV is empirically highly predictive for low grade brain tumor in the pediatric population, while a T2*-dominant or baseline pattern has high sensitivity for a high grade tumor. In addition to rCBV data [2], TSITCs from DSC perfusion potentially offers additional information not otherwise apparent with routine anatomic MRI sequences. Recognition of a T1-dominant leakage pattern may improve accuracy in preoperatively predicting the presence of a low grade pediatric brain tumor. While experienced pediatric neuroradiologists can recognize low versus high grade tumors in the majority of cases, recognition of this pattern of perfusion leakage may be highly helpful in the minority of cases where low grade pilocytic or pilomyxoid astrocytomas become large and heterogeneous, mimicking higher grade neoplasms and conversely, when high grade astrocytomas have benign imaging features (Figures 1, 2). Furthermore, when complete surgical resection is not possible, knowing the likelihood of a high grade or low grade tumor can guide how aggressive a neurosurgeon should be in debulking the tumor, at the risk of significant morbidity and mortality.

Limitations

The neuroradiologists evaluating the perfusion data were not blinded to the anatomic MRI sequences, some of which were highly suggestive of the tumor diagnosis. This was unavoidable because the anatomic images provide information integral in the assessment of the perfusion images (e.g. location of tumor, location of major vessels, etc.) This limitation is reasonable however, because it reflects the process in which MR perfusion images are evaluated in clinical practice. As noted in the discussion, a T1-dominant contrast leakage pattern has been described in CNS lymphoma and our series of 63 pediatric brain tumors included no cases of CNS lymphoma. While this represents a potential pitfall in using a T1-dominant leakage pattern to

classify pediatric brain tumors as low grade, CNS lymphoma is rarely encountered in the pediatric population. Contrast medium infusion rate and peripheral intravenous catheter gauge are related issues that likely affect the quality of the perfusion study and are recognized challenges with performing DSC perfusion MRI on pediatric patients [28]. However, only one study out of the 65 identified by the search criteria was excluded for poor contrast medium bolus, indicating that high quality DSC perfusion MRI can be performed in pediatric brain tumor patients. Differences in TR and TE parameters corresponded to studies obtained on different 1.5T and 3.0T scanners and theoretically has some effect on signal intensity and recovery/leakage patterns. However, our analysis demonstrates no significant differences in our results attributable to these different field strengths or parameters. It is important to note that there is no standardized criteria in the literature for T1 leak/T2* leak, or return to baseline. We arbitrarily chose the +/-10% range for the curve classification as a means of separation, and consequently curve classification could be altered if different thresholds are utilized. Similarly, as previously described, larger differences in technical parameters (flip angle, TE, TR) may result in greater differences in curve classification.

CONCLUSIONS

There is good interobserver agreement in classification of DSC perfusion tissue signal intensity time curves for pediatric brain tumors. Among our population of pediatric brain tumor patients, a T1-dominant leakage pattern is 100% specific for a low grade tumor and sensitive and specific for piloid astrocytomas, regardless of dexamethasone treatment. The addition of tissue signal intensity time curves may help in cases where low grade tumors are large and heterogeneous, mimicking high grade neoplasms.

REFERENCES

1. Ostrom QT, de Blank PM, Kruchko C, et al. **Alex's Lemonade Stand Foundation Infant and Childhood Primary Brain and Central Nervous System Tumors Diagnosed in the United States in 2007-2011**. *Neuro Oncol* 2015;16 Suppl 10:x1-x36

2. Ho CY, Cardinal JS, Kamer AP, Kralik SF. **Relative cerebral blood volume from dynamic susceptibility contrast perfusion in the grading of pediatric primary brain tumors**. *Neuroradiology* 2015;57:299-306

3. Kralik SF, Taha A, Kamer AP, et al. **Diffusion imaging for tumor grading of supratentorial brain tumors in the first year of life.** *AJNR Am J Neuroradiol* 2014;35:815-23

4. Panigrahy A, Nelson MD Jr, Blüml S. **Magnetic resonance spectroscopy in pediatric neuroradiology: clinical and research applications**. *Pediatr Radiol* 2010;40:3-30

5. de Fatima Vasco Aragao M, Law M, Batista de Almeida D et al. **Comparison of perfusion, diffusion, and MR spectroscopy between low-grade enhancing pilocytic astrocytomas and high-grade astrocytomas**. *AJNR Am J Neuroradiol*. 2014 Aug;35:1495-502

6. Law M, Yang S, Wang H, et al. **Glioma grading: sensitivity, specificity, and predictive values of perfusion MR imaging and proton MR spectroscopic imaging compared with conventional MR imaging**. *AJNR Am J Neuroradiol* 2003;24:1989-1998

7. Law M, Young R, Babb J, et al. **Histogram analysis versus region of interest analysis of dynamic susceptibility contrast perfusion MR imaging data in the grading of cerebral gliomas**. *AJNR Am J Neuroradiol* 2007;28:761-766

8. Morita N, Wang S, Chawla S, et al. **Dynamic susceptibility contrast perfusion weighted imaging in grading of nonenhancing astrocytomas**. *J Magn Reson Imaging* 2010;32:803-8

9. Mangla R, Kolar B, Zhu T, et al. **Percentage signal recovery derived from MR dynamic susceptibility contrast imaging is useful to differentiate common enhancing malignant lesions of the brain**. *AJNR Am J Neuroradiol* 2011;32:1004–10

10. Hartmann M, Heiland S, Harting I, et al. **Distinguishing of primary cerebral lymphoma from high-grade glioma with perfusion-weighted magnetic resonance imaging**. *Neurosci Lett* 2003;338:119–22

11. Sugahara T, Korogi Y, Shigematsu Y, et al. **Perfusion-sensitive MRI of cerebral lymphomas: a preliminary report**. *J Comput Assist Tomogr* 1999;23:232–237

12. Hu LS, Baxter LC, Pinnaduwage DS, et al. **Optimized preload leakage-correction methods to improve the diagnostic accuracy of dynamic susceptibility-weighted contrast-enhanced perfusion MR imaging in posttreatment gliomas**. *AJNR Am J Neuroradiol* 2010;31:40-48

13. Kassner A, Annesley DJ, Zhu XP, et al. **Abnormalities of the contrast re-circulation phase in cerebral tumors demonstrated using dynamic susceptibility contrast-enhanced imaging: a possible marker of vascular tortuosity**. *J Magn Reson Imaging* 2000;11:103–13

14. Jackson A, Kassner A, Annesley-Williams D, et al. **Abnormalities in the recirculation phase of contrast agent bolus passage in cerebral gliomas: comparison with relative blood volume and tumor grade**. *AJNR Am J Neuroradiol* 2002;23:7–14

15. Paulson ES, Schmainda KM. **Comparison of dynamic susceptibility-weighted contrast-enhanced MR methods: recommendations for measuring relative cerebral blood volume in brain tumors**. *Radiology* 2008;249:601–13

16. Boxerman JL, Paulson ES, Prah MA, Schmainda KM. **The effect of pulse sequence parameters and contrast agent dose on percentage signal recovery in DSC-MRI: implications for clinical applications**. *AJNR Am J Neuroradiol* 2013;34:1364-9

17. Cha S, Lupo JM, Chen MH, et al. **Differentiation of glioblastoma multiforme and single brain metastasis by peak height and percentage of signal intensity recovery derived from dynamic susceptibility-weighted contrast-enhanced perfusion MR imaging**. *AJNR Am J Neuroradiol* 2007;28:1078-84

18. Grand SD, Kremer S, Tropres IM, et al. **Perfusion-sensitive MRI of pilocytic astrocytomas: initial results**. *Neuroradiology* 2007;49:545-50

19. Cha S. **Dynamic susceptibility-weighted contrast-enhanced perfusion MR imaging in pediatric patients**. *Neuroimaging Clin N Am* 2006;16:137-147

20. Koeller KK, Rushing EJ. **From the archives of the AFIP: pilocytic astrocytoma: radiologic-pathologic correlation**. *Radiographics* 2004;24:1693–708

21. Chikai K, Ohnishi A, Kato T, et al. **Clinico-pathological features of pilomyxoid astrocytoma of the optic pathway**. *Acta Neuropathol* 2004;108:109–114

22. Ceppa EP, Bouffet E, Griebel R, et al. **The pilomyxoid astrocytoma and its relationship to pilocytic astrocytoma: report of a case and a critical review of the entity**. *J Neurooncol* 2007;81:191–196

23. Jeon YK, Cheon JE, Kim SK et al. **Clinicopathological features and global genomic copy number alterations of pilomyxoid astrocytoma in the hypothalamus/optic pathway: comparative analysis with pilocytic astrocytoma using array-based comparative genomic hybridization**. *Mod Pathol* 2008;21:1345-56

24. Brat DJ, Scheithauer BW, Fuller GN, Tihan T. **Newly codified glial neoplasms of the 2007 WHO Classification of Tumours of the Central Nervous System: Angiocentric glioma, pilomyxoid astrocytoma and pituicytoma**. *Brain Pathol* 2007;17:319–324

25. Johnson MW, Eberhart CG, Perry A, et al. **Spectrum of pilomyxoid astrocytomas: intermediate pilomyxoid tumors**. *Am J Surg Pathol* 2010;34:1783-91

26. Jarden JO, Dhawan V, Moeller JR et al. **The time course of steroid action on blood-to-brain and blood-to-tumor transport of 82Rb: a positron emission tomographic study**. *Ann Neurol* 1989;25:239-45

27. Sinha S, Bastin ME, Wardlaw JM et al. **Effects of dexamethasone on peritumoural oedematous brain: a DT-MRI study**. *J Neurol Neurosurg Psychiatry* 2004;75:1632-5

28. Yeom KW, Mitchell LA, Lober RM, et al. **Arterial Spin-Labeled Perfusion of Pediatric Brain Tumors**. *AJNR Am J Neuroradiol* 2014;35:395-401

	Cases	Age (years)		Tissue Signal Intensity Time Curve (TSITC) Classification		
		Average	Range	T1	Baseline	T2
All cases	63	6.3	1.0 - 16.8	25	23	15
Infratentorial	39	5.6	1.2 - 14.2	16	13	10
Supratentorial	24	7.4	1.0 - 16.8	9	10	5
WHO 1	25	7.1	1.1 - 15.0	18	5	2
WHO 2	13	5.9	1.2 - 16.8	7	3	3
WHO 3	9	4.6	1.4 - 12.0	0	6	3
WHO 4	16	6.4	1.0 - 16.2	0	9	7
Pilocytic astrocytoma	17	7.3	2.2 - 15.0	15	1	1
Medulloblastoma	9	6.8	2.3 - 13.3	0	4	5
Ependymoma WHO 3	7	4.3	1.4 - 12.0	0	4	3
Pilomyxoid astrocytoma	6	2.9	1.2 - 5.8	6	0	0
Ependymoma WHO 2	3	2.2	1.5 - 2.9	1	0	2
ATRT	3	1.4	1.0 - 1.9	0	3	0
GBM	3	6.9	4.2 - 9.5	0	2	1
Choroid plexus papilloma	2	4.1	3.1 - 5.2	1	1	0
Fibrillary astrocytoma	1	4.3		0	1	0
Craniophayngioma	1	5.5		0	1	0
Desmoplastic infantile ganglioglioma	1	1.1		1	0	0
Ganglioglioma	1	12.9		0	1	0
Ganglion cell tumor	1	1.8		0	1	0
High grade diffuse glioma	1	6.9		0	1	0
Low grade glioma	1	12.8		0	0	1
Low grade glioneuronal tumor	1	11.5		1	0	0
Low-grade oligoastrocytoma	1	16.8		0	1	0
Oligodendroglioma	1	15.5		0	1	0
Pineal parenchymal tumor WHO 2	1	15.6		0	0	1
Supratentorial PNET	1	16.2		0	0	1
Anaplastic astrocytoma	1	4		0	1	0

Table 1. Tumor pathology with patient age and TSITC results.

	Sensitivity	Specificity	PPV	NPV
T1 leakage pattern for low grade tumors	**66% (49-80%)** *79% (57-92%)* 43% (19-70%)	**100% (83-100%)** *100% (77-100%)* 100% (60-100%)	**100% (83-100%)** *100% (79-100%)* 100% (52-100%)	**66% (49-80%)** *77% (54-91%)* 50% (26-74%)
T2* leakage and baseline patterns for high grade tumors	**100% (83-100%)** *100% (77-100%)* 100% (60-100%)	**66% (49-80%)** *79% (57-92%)* 43% (19-70%)	**66% (49-80%)** *77% (54-91%)* 50% (26-74%)	**100% (83-100%)** *100% (79-100%)* 100% (52-100%)
T1 leakage for pilocytic and pilomyxoid astrocytomas	**91% (70-98%)** *94% (69-100%)* 83% (36-99%)	**90% (75-97%)** *88% (67-97%)* 94% (68-100%)	**84% (63-95%)** *84% (60-96%)* 83% (36-99%)	**95% (81-99%)** *95% (75-100%)* 94% (68-100%)

Table 2. Diagnostic sensitivity of leakage patterns and tumors with 95% confidence intervals. PPV = positive predictive value. NPV = Negative predictive value. All tumors results are bolded, dexamethasone tumors results are italicized, and non-dexamethasone tumors results are normal font.

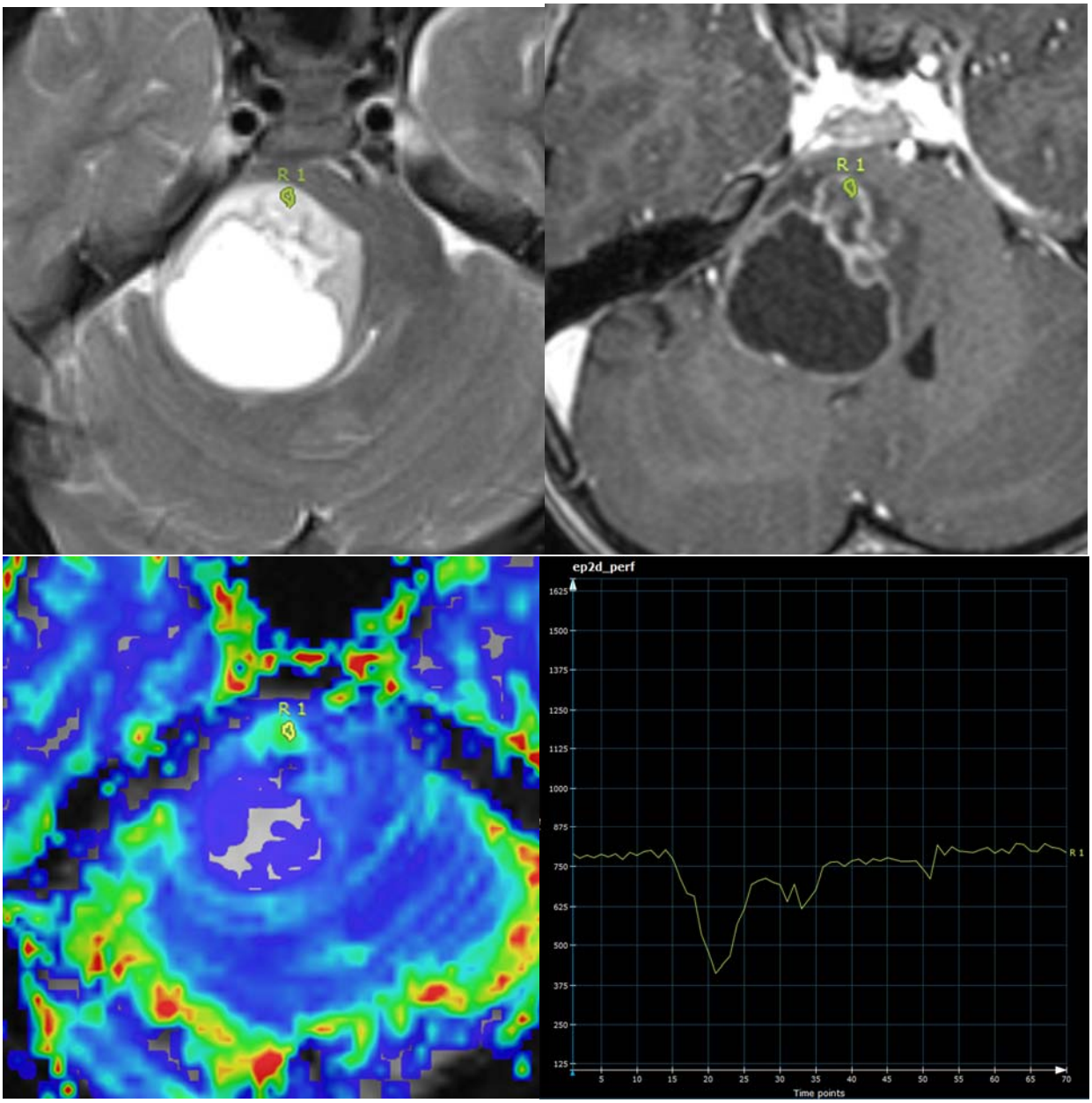

Figure 1. Axial T2 (A), axial T1 weighted post contrast (B), axial DSC perfusion CBV map (C), and tissue signal time intensity curve (D) of a glioblastoma. The tumor has T2 hyperintensity, cystic change, minimal heterogeneous enhancement and has well circumscribed margins suggesting a low grade neoplasm such as a pilocytic astrocytoma. However, the TSITC from a ROI with the highest tumoral rCBV demonstrates a return to baseline pattern, which is highly sensitive for a high grade tumor, and low probability that this represents a pilocytic or pilomyxoid astrocytoma.

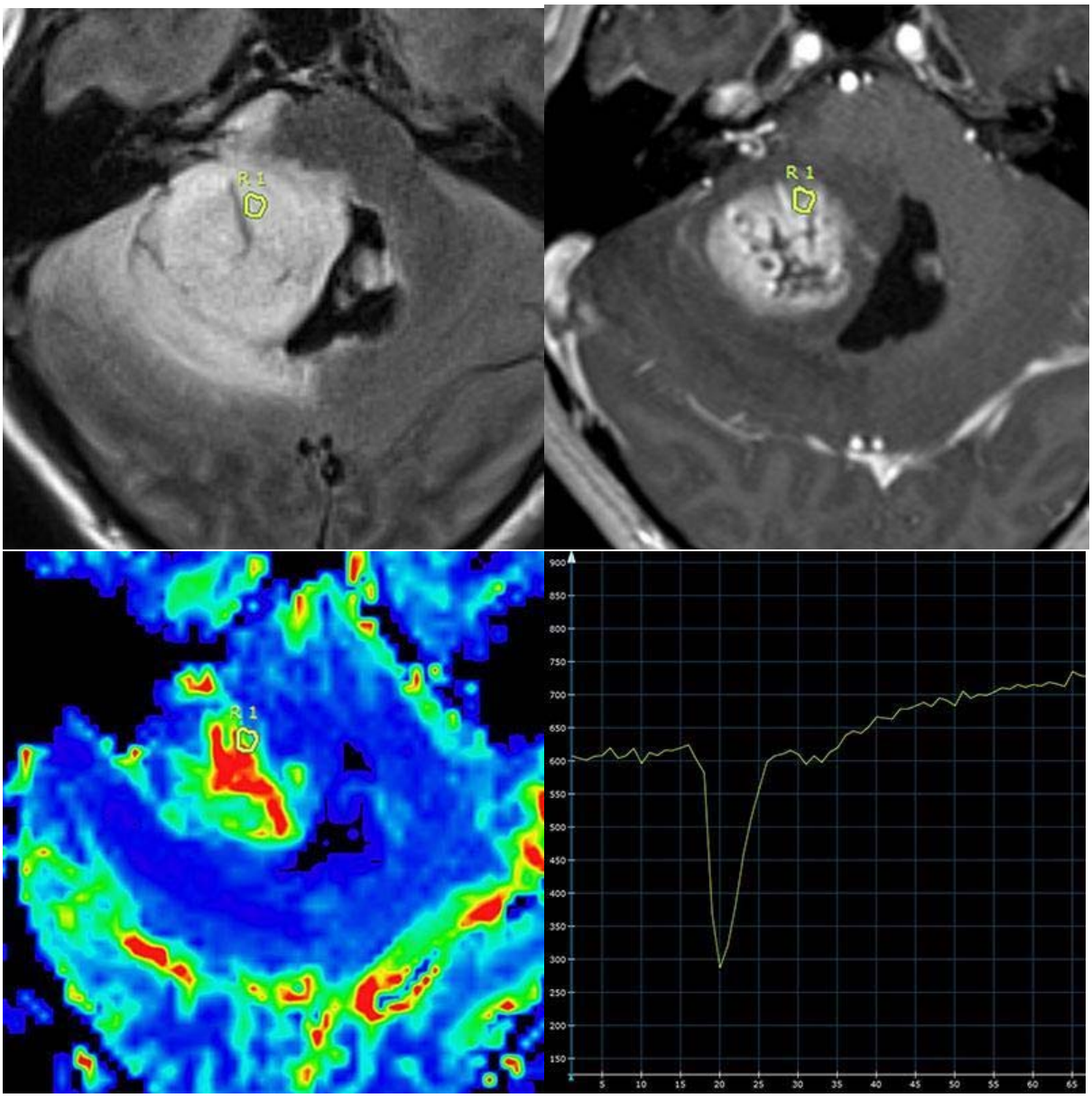

Figure 2. Axial T2 FLAIR (A), axial T1-weighted post contrast (B), axial DSC perfusion rCBV map (C), and tissue signal intensity time curve (D) of a pilocytic astrocytoma with atypical appearance. Despite apparent increased rCBV, poorly defined margins, central necrosis and surrounding T2 hyperintensity suggesting a high grade neoplasm, the T1-dominant leakage pattern suggests the correct interpretation of a low grade tumor. The ROI is placed in the highest perfusing portion of the tumor not including a dominant central vessel.

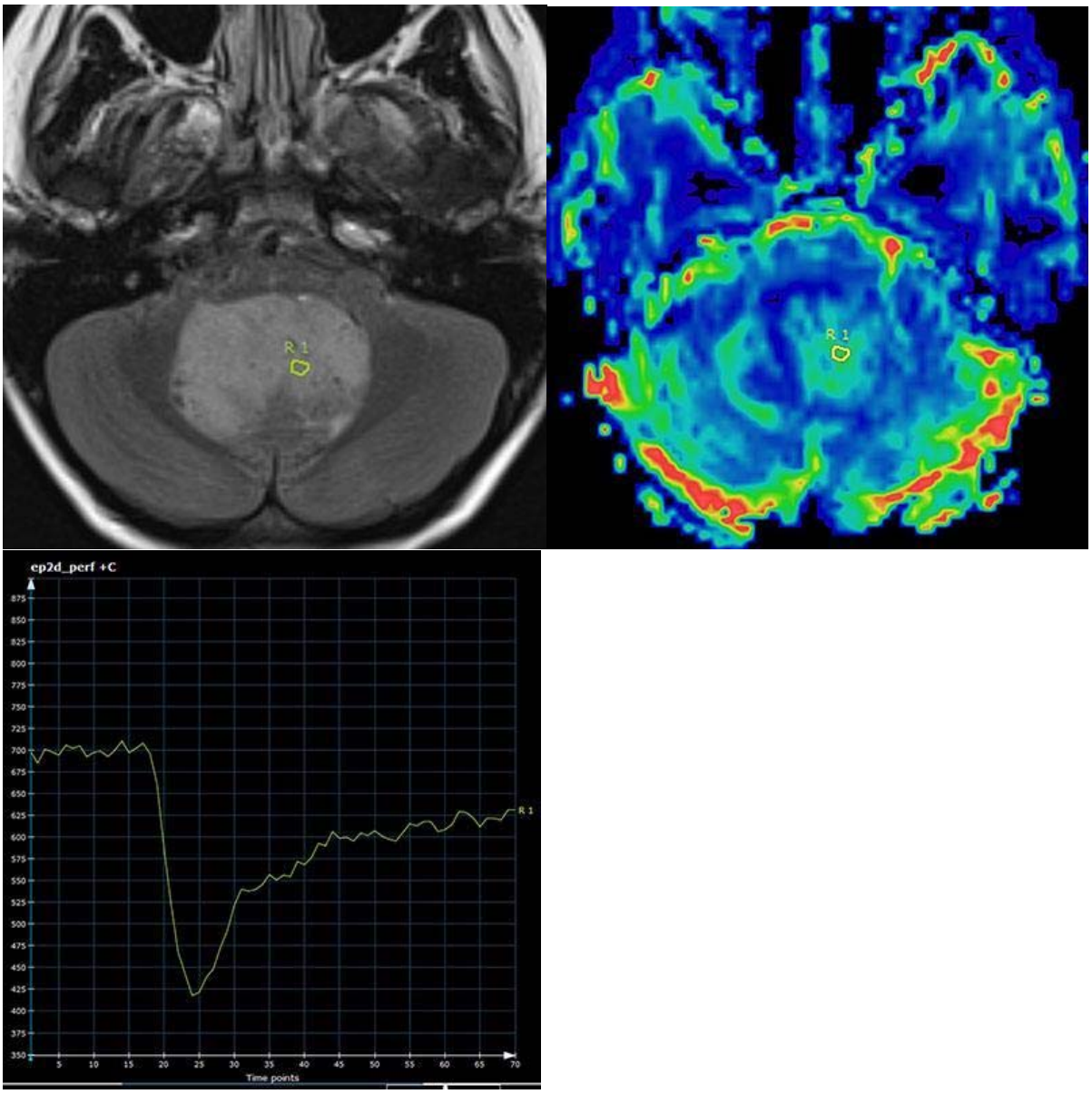

Figure 3. Axial T2 FLAIR (A), axial DSC perfusion rCBV map (B), and tissue signal intensity time curve (C) in a patient with medulloblastoma. The tissue signal intensity time curve demonstrates T2*-dominant contrast leakage following the contrast bolus.